High-Throughput DNA sequencing of ancient wood

Stefanie Wagner, Frédéric Lagane, Andaine Seguin-Orlando, Mikkel Schubert,
Thibault Leroy, Erwan Guichoux, Emilie Chancerel, Inger Bech-Hebelstrup,
Vincent Bernard, Cyrille Billard, et al.

High-Throughput DNA sequencing of ancient wood

Stefanie Wagner,[1,2,3]* Frédéric Lagane,[1] Andaine Seguin-Orlando,[2] Mikkel Schubert,[2] Thibault Leroy,[1] Erwan Guichoux,[1] Emilie Chancerel,[1] Inger Bech-Hebelstrup,[4] Vincent Bernard,[5] Cyrille Billard,[6] Yves Billaud,[7,8] Matthias Bolliger,[9] Christophe Croutsch,[10,11] Katarina Čufar,[12] Frédérique Eynaud,[13] Karl Uwe Heussner,[14] Joachim Köninger,[15] Fabien Langenegger,[16] Frédéric Leroy,[17] Christine Lima,[17] Nicoletta Martinelli,[18] Garry Momber,[19] André Billamboz,[20] Oliver Nelle,[20] Antoni Palomo,[21] Raquel Piqué,[21] Marianne Ramstein,[9] Roswitha Schweichel,[22] Harald Stäuble,[23] Willy Tegel,[24] Xavier Terradas,[25] Florence Verdin,[26] Christophe Plomion,[1] Antoine Kremer,[1]†* and Ludovic Orlando[2,3]†

[1]BIOGECO, INRA, University of Bordeaux, 33620 Cestas, France. [2]Centre for GeoGenetics, Natural History Museum of Denmark, University of Copenhagen, 1350 Copenhagen, Denmark. [3]Laboratoire AMIS, CNRS UMR 5288, Université Paul Sabatier (UPS), 31000 Toulouse, France. [4]Museum Lolland Falster, 4800 Nykøbing Falster, Denmark. [5]Dendro-Archaeology, CNRS, UMR 6566 CReAAH, University of Rennes, 35042 Rennes cedex, France. [6]DRAC Basse Normandie, 61000 Alençon, France. [7]MCC/DRASSM, 13016 Marseille, France. [8]Edytem, University of Savoie, 73376 Le Bourget-du-Lac, France. [9]Siedlungs- und Unterwasserarchäologie, Amt für Kultur/Archäologischer Dienst, 3001 Bern, Switzerland. [10]Archéologie Alsace 11, 67600 Sélestat, France. [11]UMR 7044 ARCHIMEDE, 67083 Strasbourg Cedex, France. [12]Biotechnical Faculty, Department of Wood Science and Technology, University of Ljubljana, SI-1000 Ljubljana, Slovenia. [13]Laboratoire EPOC, UMR 5805, University of Bordeaux, 33615 Pessac, France. [14]Deutsches Archäologisches Institut, Zentrale, Referat Naturwissenschaften/Dendrochronologie, 14195 Berlin, Germany. [15]Janus Verlag Freiburg im Breisgau, 79100 Freiburg im Breisgau, Germany. [16]Laténium, Museum of Archaeology, 2068 Hauterive, Switzerland. [17]Département des Recherches Archéologiques Subaquatiques et Sous-Marines, 13016 Marseille, France. [18]Dendrodata s.a.s., 37126 Verona, Italy. [19]Maritime Archaeology Trust, National Oceanography Centre, Southampton SO14 3ZH, United Kingdom. [20]Baden-Wuerttemberg State Office for Cultural Heritage, Tree-ring Lab, 78343 Hemmenhofen, Germany. [21]Universitat Autònoma de Barcelona, 08193 Bellaterra, Spain. [22]Amt fuer Archaeologie im Thurgau, 8510 Frauenfeld, Switzerland. [23]Landesamt fuer Archaeologie, 01109 Dresden, Germany. [24]Institute for Forest Growth, University of Freiburg, Germany. [25]Spanish National Research Council. IMF - Archaeology of Social Dynamics. Barcelona, Spain. [26]CNRS, UMR 5607 Ausonius, Maison de l'Archéologie, 33607 Pessac cedex, France.

† These authors are joint last authors

* These authors are the corresponding authors: stefanie.wagner@inra.fr; antoine.kremer@inra.fr

Abstract

Reconstructing the colonization and demographic dynamics that gave rise to extant forests is essential to forecasts of forest responses to environmental changes. Classical approaches to map how population of trees changed through space and time largely rely on pollen distribution patterns, with only a limited number of studies exploiting DNA molecules preserved in wooden tree archaeological and subfossil remains. Here, we advance such analyses by applying high throughput (HTS) DNA sequencing to wood archaeological and subfossil material for the first time, using a comprehensive sample of 167 European white oak waterlogged remains spanning a large temporal (from 550 to 9,800 years) and geographical range across Europe. The successful characterization of the endogenous DNA and exogenous microbial DNA of 140 (~83%) samples helped the identification of environmental conditions favoring long-term DNA preservation in wood remains, and started to unveil the first trends in the DNA decay process in wood material. Additionally, the maternally-inherited chloroplast haplotypes of 21 samples from three periods of forest human-induced use (Neolithic, Bronze Age and Middle Ages) were found to be consistent with those of modern populations growing in the same geographic areas. Our work paves the way for further studies aiming at using ancient DNA preserved in wood to reconstruct the micro-evolutionary response of trees to climate change and human forest management.

Introduction

Forests cover 31% of the land area worldwide and are among the most biologically-rich and genetically-diverse ecosystems on the planet (MacDicken 2015). Reconstructing the evolutionary dynamics that gave rise to the current distribution patterns of long-lived sessile organisms, such as trees, is challenging, but essential to understand how these ecosystems respond to environmental change (Aitken *et al.* 2008; Franks *et al.* 2014). Classically, the postglacial recolonization routes of trees from glacial refugia have been documented with large-scale pollen, macrofossil and modern genetic data (Petit *et al.* 2002b; Cheddadi *et al.* 2006; Magri 2008; Tollefsrud *et al.* 2008; Liepelt *et al.* 2009; Wagner *et al.* 2015b). In addition, environmental DNA has been used as a complementary

proxy and opened new possibilities for the reconstruction of past forest communities applying high-throughput DNA sequencing (HTS) on sedimentary time series (Jørgensen *et al.* 2012; Parducci *et al.* 2012; Giguet-Covex *et al.* 2014; Smith *et al.* 2015; Pedersen *et al.* 2016; Schmid *et al.* 2017). Ancient DNA (aDNA) from wood material has also been investigated, but to a much more limited extent, with only a handful of studies hitherto reported (Tani *et al.* 2003; Pollmann *et al.* 2005; Deguilloux *et al.* 2006; Liepelt *et al.* 2006; Speirs *et al.* 2009; Gómez-Zeledón *et al.* 2017; Lendvay *et al.* 2017). These have relied on a methodological framework including the amplification of short PCR fragments and/or metabarcodes, real-time PCR and sequencing, including, for the most recent study, amplicon-sequencing on Illumina platforms (Lendvay *et al.* 2017). They have not yet explored the full potential of aDNA methods based on shotgun HTS, which have now become almost routine for the study of the genome-scale variation present in ancient animals and pathogens (Orlando *et al.* 2015).

Subfossil (non-petrified) wood logs and archaeological timber from temperate Europe are ubiquitous and, ancient DNA apart, have been extensively studied in a range of scientific areas, including paleoclimatology, dendrochronology and dendroarchaeology (Becker *et al.* 1991; Friedrich *et al.* 1999; Becker 2006; Büntgen *et al.* 2011; Billamboz 2014). Wood can be dated at a one-year resolution from tree-ring patterns, allowing the reconstruction of detailed history of forest cover changes, including natural vegetation succession and human exploitation (Čufar *et al.* 2010; Martinelli 2013; Billamboz 2014). Archaeological wood samples with exceptionally well-preserved morphological features have been excavated from waterlogged environments, such as groundwater-saturated wetlands and submerged archaeological layers within lakes and oceans (Čufar *et al.* 2010; Aguilera *et al.* 2011; Tegel *et al.* 2012; Martinelli 2013). In that regard, the prehistoric pile dwellings around the Alps, more than 800 of which have been classified as World Heritage sites by UNESCO (http://sites.palafittes.org/), constitute a unique archive for studying forest changes with large numbers of trees spanning multiple generations since the Neolithic period. Equally well-preserved subfossil logs corresponding to assemblies of submerged tree trunks have been reported from European foreshores and alluvial gravel pits (Friedrich *et al.* 2004; Nayling *et al.* 2007). However, after excavation, waterlogged wood decays very rapidly and little is known about the underlying microbial

taxa, which have mostly been characterized by microscopy and spectroscopy (Pedersen 2015), but extremely limited by DNA studies (Palla *et al.* 2014). The application of DNA-based molecular methods unveiling the microbiota associated with specific environmental requirements and/or degradation pathways may help facilitate both future aDNA analyses of waterlogged wood material and strategies for the *ex situ* and *in situ* conservation of waterlogged wooden cultural heritage items.

A number of studies have explored the potential of waterlogged environments for DNA preservation within plant remains of various types, including pips and seeds (Tani *et al.* 2003; Pollmann *et al.* 2005; Liepelt *et al.* 2006; Speirs *et al.* 2009; Schlumbaum *et al.* 2012; Wales *et al.* 2014, 2016; Gómez-Zeledón *et al.* 2017) 2017), and showed limited success on waterlogged wood (Tani *et al.* 2003; Pollmann *et al.* 2005; Deguilloux *et al.* 2006; Liepelt *et al.* 2006; Speirs *et al.* 2009). The methodology underlying all previous DNA studies of waterlogged wood relied on the PCR amplification of pre-selected DNA markers, and was not tailored to the molecular characteristics of ancient DNA, the vast majority of which consisting of ultra-short, degraded DNA molecules (Orlando *et al.* 2015). Additionally, dead cells are predominant in the heartwood (i.e. the inner part of the tree trunk), limiting the available amount of DNA molecules. Furthermore, wood material is notorious for containing large amounts of secondary metabolites and other inhibitory compounds hampering DNA experiments (Plomion *et al.* 2001; Deguilloux *et al.* 2002). It thus remains unclear whether the limited success of previous studies reflects methodological limitations or the poor potential for DNA preservation in waterlogged wood remains.

Here, we focused on two temperate trees, the pedunculate oak (*Quercus robur*) and the sessile oak (*Quercus petraea*). These two species are distributed across Europe and are represented by extensive paleontological and archaeological records, including wood remains compatible with dendrochronological dating (Becker *et al.* 1991; Friedrich *et al.* 2004; Becker 2006). The two species share multiple maternally-inherited chloroplast haplotypes (Petit *et al.* 2002a; Kremer *et al.* 2002), and species assignment requires appropriate diagnostic nuclear markers (Muir *et al.* 2000; Guichoux *et al.* 2011). The modern distribution of the chloroplast haplotypes is geographically structured and

has been studied based on more than 2600 modern populations (Petit *et al.* 2002a; b), providing a valuable reference for comparisons with ancient haplotypes. Oaks have long life expectancies (~500-800 years) and generation times (~30-80 years) (Lang 1994), and estimates of substitutions rates in chloroplast DNA within the Fagaceae family are low in comparison to other angiosperms, with substitution rates in the order of 10^{-10} substitutions per nucleotide per year (Frascaria *et al.* 1993). The presence in a given area of haplotypes otherwise characteristic of other geographical regions can thus be used with confidence to track recent migrations and/or anthropogenic translocations across different parts of the range (König *et al.* 2002; Lowe *et al.* 2004).

In this study, we applied HTS to aDNA extracts prepared from 167 subfossil and archaeological waterlogged samples of oak wood remains (*Quercus robur/petraea*), excavated from diverse environmental and taphonomical contexts across Europe and spanning the whole Holocene (Fig. 1, Table 1, Table S 1). We characterized aDNA preserved in waterlogged wood, identified potential environmental key factors favoring its preservation, uncovered DNA decay kinetics and tracked maternal haplotypes through time focusing on periods of human forest-use. This work paves the way for large-scale evolutionary studies on trees based on ancient organelle and nuclear DNA preserved in wood.

Materials and Methods

Samples. We collected 167 waterlogged wood samples from 26 sites spread across Spain, France, Switzerland, Italy, Slovenia, Germany, England and Denmark. These encompass a range of taphonomical and temporal (500 to 9,800 years) contexts (Fig. 1, Table 1) dated by dendrochronology and/or radiocarbon methods (Table S 1). Taxonomic resolution was limited to the *Quercus robur/petraea* level due to the close wood anatomical features present in both species (Schweingruber 1990). To increase the amount of initial DNA, we collected only samples with preserved sapwood (i.e. the outer, formerly functional part of the wood) (Plomion *et al.* 2001; Deguilloux *et al.* 2002). The wood remains from archaeological structures (e.g. pile dwellings, water

wells, fish weirs) and subfossil logs sampled were waterlogged and located in ground- or seawater-saturated wetlands or submerged in lakes or oceans. We gathered at least four samples from each site, except for Reims and Unteruhldingen site 1, for which only three samples could be studied. Most samples had been excavated within the last three years, but we also included 47 additional samples, which were part of earlier collections, in order to increase the temporal and spatial resolution. We note that the samples collected at Bouldnor Cliff consist of subfossil tree remains especially excavated from two new sampling localities, representing submerged peats rich in wooden macro-remains, and did not consist of sedimentary cores, in contrast to previous work (Smith *et al.* 2015; Weiß *et al.* 2015; Kistler *et al.* 2015). We reconstructed the storage conditions for all sites, including the archived samples (Table 1, Table S 1). At 14 sites, the samples were vacuum-packed and stored at +4°C immediately after their excavation, to minimize molecular degradation.

DNA extraction, library construction and sequencing. DNA extraction, library construction and PCR were performed at the dedicated ancient DNA facilities of the Centre for GeoGenetics, University of Copenhagen, Denmark. We focused on sapwood and combined previously published DNA extraction protocols (Cappellini *et al.* 2010; Wales *et al.* 2012; Gamba *et al.* 2016) to maximize DNA recovery. Our procedure consisted of the following seven steps: (1) removal of the external surface with sterile scalpels, (2) grinding of $1x1x0.2$ cm^3 humid wood cuboids in sterile mortars, (3) digestion of the resulting wood paste at 37°C for 20 h in 3 mL lysis buffer consisting of 10 mM Tris-HCl, 10 mM NaCl, 2% w/v SDS, 5 mM CaCl$_2$, 2.5 mM EDTA, 40 mM DTT and 10% proteinase K, (4) extraction of DNA twice in phenol and then once in chloroform, (5) mixing of the DNA supernatant with 3 mL Tris-EDTA (1X), (6) concentration on Amicon Ultra 4 (30 kD) filters and (7) purification on MinElute PCR purification columns (QIAGEN, Hilden, Germany). For five samples, pairwise comparisons of the DNA extraction yields for sapwood and heartwood material were carried out. We expected higher DNA yields in sapwood, given the higher proportion of living cells present in this material relative to heartwood. We treated 13 DNA extracts with the USER enzyme mixture (uracil–DNA–glycosylase and endonuclease VIII), as described by Gamba *et al. (2016)*, before DNA library construction, amplification and sequencing, with the aim of achieving a minimum of 8X

coverage of the chloroplast genome.

DNA libraries were constructed by blunt-end DNA ligation, with 16 μL of DNA solution, in a final volume of 25 μL, as described by Meyer and Kircher (2010) and Gamba *et al*. (2016). DNA library concentration was assessed by real-time PCR (Roche Light Cycler 480) and SYBR Green chemistry. Real-time PCR was performed in duplicate, with a 20 μL reaction volume consisting of 1 μL 1:20-diluted library, 0.1 U/μL TaqGold (Invitrogen, Life Technologies), 1X Gold Buffer, 4 mM $MgCl_2$, 1 mg/mL BSA, 1 mM dNTPs, 0.2 mM Illumina in PE1.0 primer (5′-AAT GAT ACG GCG ACC ACC GAG ATC TAC ACT CTT TCC CTA CAC GAC GCT CTT CCG ATC T) and 0.2 mM Multiplex Index Primer (5'- CAA GCA GAA GAC GGC ATA CGA GAT NNN NNN GTG ACT GGA GTT CAG ACG TGT GCT CTT CCG), where NNN NNN is a unique, 6-mer index tag. Amplification conditions were set as follows: 10 minutes at 92°C (initial activation by heating), 40 cycles of 30 seconds at 92°C (denaturation), 30 seconds at 60°C (annealing) and 30 seconds at 72°C (elongation), and then 7 minutes at 72°C (final elongation). We determined Ct values with the second-derivative maximum algorithm implemented in LightCycler software. Indexing PCR was performed in the same conditions as real-time PCR, except that the final volume was 25 μL, the volume of undiluted library used was 4 μL, and the number of amplification cycles was set at the previously determined Ct value minus 5, to correct for dilution effects. PCR products were purified on MinElute columns (QIAGEN, Hilden, Germany), in a final volume of 25 μL and were diluted 1:10 for quantification on a 2200 TapeStation instrument (Agilent Technologies) with High-Sensitivity ScreenTape D1000 reagents (Agilent Technologies). Libraries were then pooled and shotgun-sequenced at the Danish National High-Throughput Sequencing Centre, on a HiSeq2500 instrument, with 100 single-end cycles.

Contamination control. Blank controls were included in all laboratory steps and were analyzed in parallel with the samples. They encompassed extraction blank controls (EBC), library blank controls (LBC), PCR controls (qPBC) and an indexing blank control (iPBC). For real-time PCR quantification, the Ct value obtained for blank controls was at least 10 cycles greater than that for the samples. Assuming a reaction efficiency of 100%, this limits the maximal contamination level to 0.1% (Table

S 2). Blank controls were also PCR-indexed with the maximum number of cycles observed across the experimental sample sets, but negative profiles were obtained on the TapeStation instrument.

Endogenous and exogenous DNA content. Raw reads were demultiplexed based on exact index match. We mapped the sequencing reads independently against a haploid version of the *Quercus robur* reference genome (740 Mb/C: Plomion *et al.* (2016) Leroy *et al.* (2017)), using PALEOMIX (Schubert *et al.* 2014), with the bwa-backtrack algorithm within the Burrows-Wheeler Aligner (Li *et al.* 2009). Seeding was disabled as per the recommendations from Schubert and colleagues (Schubert *et al.* 2012) and alignments with a mapping quality below 25, unmapped reads and PCR duplicates were discarded. The same procedure was repeated for identifying chloroplast DNA reads, using the chloroplast genome as a reference (160 kb: https://w3.pierroton.inra.fr/QuercusPortal/index.php?p=GENOMIC_SEQ). Independent alignment of DNA reads against the nuclear and organellar genomes has been previously recommended to avoid alternative hits in the nuclear genome due to the presence of nuclear organellar insertions (such as numts, for mitochondrial DNA). Such an alignment strategy can, however, result in the alignment against the organellar genome of divergent reads pertaining to nuclear organellar insertions and inflate heterozygosity levels. The limited heterozygosity levels observed on the haploid chloroplast genomes ruled out any significant impact of nuclear organellar insertions on the reconstructed chloroplast genomes (Fig. S 1). Endogenous DNA content was calculated as the fraction of high-quality nuclear and chloroplast sequences identified within the pool of sequences left after adapter trimming, quality filtering, and PCR duplicate removal. Fragment size distributions were approximated from the size distribution of high-quality read alignments. We note that the latter provides an under-estimate of the true size distribution of ancient DNA fragments, given that the full length of any template larger than 100 nucleotides cannot be determined from 100 cycle Single-End sequencing reactions. However, we note that extent of the size bias is extremely limited for the vast majority of the samples analysed, given that most aligned reads are extremely short, with the fraction of reads longer than 95 nucleotides generally representing ~0.6% (median, nuclear sequences) of the aligned reads (Fig. S 2).

Trimmed single-end reads were further processed against the MetaPhlAn2 database (Segata *et al.* 2012; Truong *et al.* 2015), including sequences from eukaryotes and viruses, with metaBIT (Louvel *et al.* 2016), to assess the exogenous microbial diversity captured within our samples. Reads were aligned with BOWTIE2 v2.1.0 (Langmead & Salzberg 2012), and the microbial composition of each sample was visualized with a range of graphical outputs provided by metaBIT, including Bray-Curtis distances (Truong *et al.* 2015; https://bitbucket.org/nsegata/hclust2/; Louvel *et al.* 2016). Shannon indices were calculated with the exclusion of taxa with an abundance <1% and fewer than 1,000 hits. Finally, the linear discriminant analysis effective size (LEfSe) method (Segata *et al.* 2011; Louvel *et al.* 2016) was run to identify and quantify the microbial taxa driving significant differences between predefined clusters identified in the principal coordinate analysis. The LEfSe analysis used default settings (non-parametric Kruskal Wallis rank-sum test, unpaired Wilcoxon test with *p*-values of 0.05, and threshold values of 2 for the logarithmic LDA score).

Authenticity. We checked that the DNA obtained was authentic by assessing DNA fragmentation and nucleotide misincorporation patterns for nuclear and chloroplast DNA, with mapDamage2.0 (Jónsson *et al.* 2013; Schubert *et al.* 2014). For samples with at least 1,000 unique hits per target genome, we quantified deamination levels in DNA overhangs (δs), with mapDamage2.0 (Jónsson *et al.* 2013). This parameter was used as a proxy for post-mortem DNA degradation and, together with average fragment lengths, was plotted against thermal age. Thermal age values were calculated with the thermal age webtool (http://thermal-age.eu/) (Table S 1), which defines thermal age as the time necessary to produce a given degree of DNA degradation at a constant temperature of +10°C (Smith *et al.* 2003). The model inputs were chronological sample age, geographic coordinates, altitude, type and thickness of the burial layers, collection year, analysis year and storage conditions (Table S 1).

Genotyping and chloroplast haplotype calling. For the 13 samples for which we had USER-treated and non-USER-treated datasets, we rescaled individual base qualities for the non-USER-treated extracts, using mapDamage2.0 (Jónsson *et al.* 2013). Rescaled read alignments were subsequently merged together with those obtained for USER-treated data with SAMtools v0.1.18 (Li *et al.* 2009).

The PALEOMIX phylo pipeline was used to reconstruct chloroplast haplotypes from 34 SNP positions known to be polymorphic within a large reference panel of ~2,600 modern haplotypes (Petit *et al.* 2002a; Guichoux & Petit 2014). The minimum read depth for genotype calls was set to four, and the minimum quality score was set to 30. Finally, the ancient haplotypes were compared with the haplotypes found in extant populations within a radius of 100 km around the study sites (Table S3). The latter were extracted from a georeferenced database storing genetic data from >3000 European white oak populations from across Europe (https://gd2.pierroton.inra.fr/gd2/login/login).

Results

Endogenous and exogenous DNA content. We recovered shotgun sequence data from the DNA extracts of 140 waterlogged sapwood samples for 24 of the 26 sampling sites. The two sites where DNA levels of all samples were equivalent to that found in extraction blanks were the Amélie foreshore and the Lillemer peatlands, where the samples were gathered from piles exposed to tides and corresponded to relatively dry logs. For the 140 samples delivering sequence data, the levels of endogenous DNA present in each individual library were found to be low, <1% for the vast majority of samples (Fig. 2, Table S4). However, endogenous DNA content was higher for 14 samples showing chronological ages between 0.5 and 5.2 thousand years (thermal ages between 0.4 and 5.6 thousand years), with unique high-quality alignments making up to 16.5% of the sequences generated (Table S 4). Interestingly, the two samples showing highest endogenous DNA content consisted of submerged piles inserted in limy lacustrine sediments from Lake Constance in southern Germany (Unteruhldingen/site 1, 3.7 thousand years, 4.8 thousand thermal years). The following samples showing high endogenous DNA levels were much younger (0.5-0.7 thousand years; 0.4-0.5 thousand thermal years) and were recovered from organic wetland sediments in northern Germany. All the other millennia-old samples with endogenous DNA contents >1% came from terrestrial and submerged limy contexts (Erstein, Eschenz-Orkopf and Sutz Lattrigen Ruette). All but one of these samples had been stored in controlled conditions (placed under vacuum and at +4°C immediately after excavation).

Read mapping against the MetaPhlAn2 database revealed the presence of diverse microbial communities, with Shannon indexes ranging from 0.05 to 3.01 (median value = 2.09; Fig. 3a, Fig. S 3, Table S 5) and 122 DNA libraries satisfying the threshold of at least 1,000 hits against the reference database. The sample with the highest endogenous DNA content displayed a predominance of the various members of the Methanomicrobia class (Fig. S 4). Principal Coordinate Analysis (PCoA) based on microbe abundances in all 122 samples (irrespective of the storage conditions) revealed no apparent structure reflecting similar environmental origins (Fig. S 5), except for samples of marine origins which projected on a closer PCoA space. However, PCoA restricted to samples stored in controlled conditions revealed clear clustering by site and/or taphonomical conditions, with the first three axes explaining more than 35% of the total variance for microbial abundance (Fig. 3b). Although additional subclusters may be present (Fig. S 6), we restricted subsequent LEfSe analyses to the four most apparent such PCoA clusters corresponding to (1) organic wetland sediments (Greifswald, Hamburg), (2) limy lake sediments (Conjux, Eschenz Orkopf, Unteruhldingen/site 1 and Unteruhldingen/site 2), (3) marine sediments (Bouldnor Cliff, Etang de Thau and Champeaux) and (4) sands and loess on limy bedrock (Erstein 208). Samples from the coastal site at Le Gurp, which had a projected position intermediate between those of clusters of marine and terrestrial sediments, were disregarded. LEfSe revealed the presence of a number of taxa driving differences in the microbial composition of the four clusters (LDA scores >3) (Fig. 3c, Fig. S 7). Samples from organic wetland sediments were particularly rich in anaerobic Methanosaetaceae, particularly *Methanosaeta concilii*, and Sphingomonadaceae, represented by *Sphingobium spec.* Marine environments were characterized by a predominance of Gammaproteobacteria, including the Shewanellaceae (*Shewanella spec., Shewanella frigidimarina*) and, typically, marine Oceaonospirillaceae and Piscirickettsiaceae. The limy soil samples were characterized by a predominance of Betaproteobacteria, including the orders of Burkholderiales (Oxalobacteraceae, *Janthinobacterium*) and Pseudomonadales (*Pseudomonas* sp*., Pseudomonas mandelii*). Finally, samples from limy lacustrine environments included families not abundant in the other environments, such as Alphaproteobacteria, Caulobacteraceae (*Caulobacter* sp., *Caulobacter vibrioides*) and other phylotypes, such as Euryarchaeota (*Methanocella* sp.). Several of

these taxa can break down lignin (e.g. *Sphingobium* spec.), cellulose (e.g. *Caulobacter* spec.) and lignin-derived aromatic molecules (e.g. *Methanosarcina* spec. *Methanocella* spec. *Rhodopseudomonas* spec.) (Taylor 1983; Harwood & Gibson 1988; Song *et al.* 2013; Tsuji *et al.* 2015; Kato *et al.* 2015).

DNA authenticity and degradation. A total number of 77 samples originating from 16 sites across Europe yielded at least 1,000 unique high-quality hits against the pedunculate oak nuclear reference genome. The thermal ages of these samples were between 0.4 and 8.7 thousand years (chronological ages between 0.5 and 5.6 thousand years). DNA fragments were of limited size, even in samples younger than 1 thousand thermal years, in which the vast majority of the endogenous DNA templates identified were shorter than 80 bp long. We found that the average size of endogenous DNA fragments tended to decrease linearly with increasing thermal age (Fig. 4a, f(x)=63.57-0.001x, r^2=0.202, p=4.05e-5). However, the magnitude of the slope of the linear model was limited and the linear model poorly explained the data observed in multiple samples, which appeared as clear outliers to the confidence range predicted by the model. Additionally, there were large size differences between samples of similar age. Altogether, this suggests that thermal age as well as additional factors, possibly related to unmodelled micro-environmental conditions, impacted on DNA fragmentation. We quantified post-mortem deamination in single-strand overhangs (δs) and found a significant correlation with thermal age until approximately 5 thousand thermal years ago (Pearson coefficient = 0.746, *p*<2e-5, Fig. 4b), when δs values reached a plateau. However, deamination was variable across samples of similar age. Nuclear and chloroplast DNA displayed the same cytosine deamination kinetics after death, as the correlation between nuclear δs and chloroplast δs values was found to be highly significant (r^2=0.992, *p*<2e-16, Fig. S 8), with a slope close to 1. In absence of significant difference between nuclear and chloroplast damage kinetics, we repeated the damage analyses, applying the threshold of 1,000 unique high-quality alignments to the sum of nuclear and chloroplast hits. This resulted in the inclusion of four additional data points (for a total of 81 samples, Fig. S 8), two of which representing samples from sites already represented in the analyses above (Unteruhldingen site 2, Conjux) and two from an additional site, the Bouldnor Cliff (Sample 523 and

524). This analysis confirmed the findings above. This analysis confirmed the findings above. Given that the authenticity of plant DNA sequences identified at the Bouldnor Cliff site has been challenged (Smith *et al.* 2015; Weiß *et al.* 2015; Kistler *et al.* 2015), it is noteworthy that the oak DNA templates identified from two of the samples from a first locality at Bouldnor Cliff (samples 523 and 524) are characterized by very small fragment sizes (<40bp), strong purine enrichment in the genomic positions preceding read start (in support of post-mortem DNA fragmentation through depurination; Briggs *et al.* 2007) and nearly maximal cytosine deamination rates within overhangs (δs=0.97). However, no evidence of cytosine deamination or depurination was found in the third sample, that was characterized by extremely small fragment sizes (<30bp). This sample comes from a second locality at Boulnor Cliff (sample 522). In absence of clear post-mortem DNA damage evidence, the data pertaining to this third sample should be taken with caution, especially given that the alignment false positive rate is likely significantly inflated for DNA fragments of such extremely limited size. We, however, note that previous work have reported limited DNA depurination levels in marine sediments (Corinaldesi *et al.* 2008) and that the differences in DNA degradation levels observed might reflect different micro-environmental conditions (and contamination rates) prevailing in the three samples and/or within the two localities investigated at Bouldnor Cliff. Some of the other archaeological sites where we analyzed multiple samples have indeed shown significant differences in DNA damage levels (Fig. 4). Further work will be needed to investigate the specific DNA degradation conditions at Bouldnor Cliff. Additional information and discussion on the Bouldnor Cliff samples compared to previous DNA results obtained for sedimentary samples (Smith *et al.* 2015) are provided as Supplementary Material (Figs S 9–S 13, Table S 6 and Text S 1).

The base composition at the genomic positions preceding read starts and following read ends were typical of ancient DNA fragmentation by depurination (Figs 4c and 4d). Typical misincorporation patterns were also observed, with higher rates of C-to-T substitution close to sequence starts, and higher G-to-A substitution rates at sequence ends (Figs 4c and 4d). This pattern indicates preferential post-mortem deamination within overhanging ends (Briggs *et al.* 2007). Finally, we compared the endogenous DNA content of libraries constructed from sapwood and heartwood extracts from five

pairs of samples. Although they were all characterized by extremely low endogenous DNA content (<0.13%, Fig. S 7), sapwood showed higher endogenous DNA levels than the heartwood in four of the five pairs of samples. This situation reflects the known, larger amounts of DNA in fresh sapwood than in heartwood (Deguilloux *et al.* 2002) and suggests that the oak DNA detected is truly endogenous, as environmental contamination would be expected to result in similar amounts in the sapwood and heartwood. This comparison adds on the evidence supporting the authenticity of our results, especially in situations where environmental conditions can hardly be controlled (e.g. sampling of wood during pollen season, uncontrolled archive conditions).

Inference of chloroplast haplotypes. The sequencing of USER- and non-USER-treated libraries led to the characterization of 21 chloroplast genomes with a mean depth-of-coverage exceeding 5X, and 11 chloroplast genomes with a mean coverage between 1X and 5X (Table 2). The nuclear coverage achieved was generally limited (<1%), except for two samples, both from Unteruhldingen/site 1 (3.7 thousand years, 4.8 thousand thermal years), where 14% nuclear coverage could be achieved using 13.5 and 10 million sequencing reads, respectively. The characterization of the complete nuclear sequence of ancient oak genomes in such samples is thus possible at a relatively reasonable cost, even in the absence of DNA library enrichment.

For the 21 samples showing chloroplast coverage >5X (0.5-5.6 thousand years, 0.4-8.7 thousand thermal years), we identified five different ancient chloroplast haplotypes from three different major lineages (Petit *et al.* 2002a): haplotypes 10 and 11 belonging to lineage B (currently spread from Spain to the British Isles), haplotype 1 belonging to lineage C (from Italy to Scandinavia) and haplotype 7 belonging to lineage A (from the Balkans to the Baltic Sea and southern France). At all sites and for all time periods considered (Neolithic, 7 haplotypes; Bronze Age, 7 haplotypes; Middle Ages, 7 haplotypes), the ancient haplotypes matched the most frequent haplotypes found in nearby extant populations (Fig. 5).

Discussion

Analyses of ancient DNA from trees can provide invaluable temporal series to investigate the response of forest ecosystems in the face of major past environmental changes. However, previous studies on ancient tree DNA have been mostly restricted to the analysis of environmental records and pollen grains (Parducci *et al.* 2005, 2012; Giguet-Covex *et al.* 2014; Willerslev *et al.* 2014; Smith *et al.* 2015; Pedersen *et al.* 2016; Schmid *et al.* 2017). The limited number of studies retrieving aDNA from wood archaeological and subfossil material were mostly based on the PCR amplification of a few candidate markers (Tani *et al.* 2003; Deguilloux *et al.* 2006; Liepelt *et al.* 2006; Speirs *et al.* 2009; Gómez-Zeledón *et al.* 2017) and most recently on amplicon-sequencing on Illumina platforms (Lendvay *et al.* 2017). They have not yet explored the full potential of aDNA methods based on shotgun HTS. In this study, we applied such a methodology for the first time to a comprehensive collection of 167 subfossil and archaeological samples of European oak (*Quercus robur/petraea*) wood remains. Our collection spans 26 sites across the whole western European range of this species assemblage (42-55°N/-2°W-15°E), and encompasses various taphonomical (terrestrial/lacustrine/marine) and temporal (0.5-9.8 thousand years) contexts.

We focused on waterlogged environments as these preserve wood material in an exceptional morphological state. By relying on sapwood, which consists of the cell-rich outer, formerly functional part of the wood, we maximized the available amount of DNA. With the molecular tools used in this study, we successfully recovered shotgun sequence data from 140 samples from 24 sites. Only two taphonomical contexts, corresponding to aerobic and/or acidic environments known to accelerate DNA decay (Collins *et al.* 2002; Smith *et al.* 2003; Nielsen-Marsh *et al.* 2007), were not amenable to DNA sequencing. Most of the sequenced samples were dominated by environmental microbial DNA, as is also generally observed in animal calcified tissues, such as bones and teeth, with the exception of petrosal bones where higher DNA preservation can be observed (Pinhasi *et al.* 2015). However, 14 samples (0.5-5.2 thousand years) had endogenous DNA contents of up to 16.5%, a value compatible with relatively cost-effective genome sequencing by shotgun sequencing.

The oak DNA samples showing the highest levels of endogenous DNA were all associated with large fractions of strictly anaerobic, methane-reducing Methanomicrobia. This suggests that anoxic conditions providing environmental conditions compatible with the survival and multiplication of such microbiota may favor the preservation of ancient DNA in waterlogged environments. We also note that all the millennia-old samples with moderate-to-high oak DNA contents (1-16.5%) originated from archaeological structures (pile dwellings, water wells) embedded in limy contexts. This suggests that such calcareous sediments could represent particularly promising environments for the preservation of ancient DNA in wooden tissues. Similar endogenous DNA contents (3-9.8%) have been obtained for archaeological samples from organic wetland deposits of neutral pH, as indicated by the molecular identification of the bacterium *Methanosaeta concilii* (pH values of 7.1-7.5). However, these samples were relatively young (<1 thousand years) and it remains unclear whether such environments are favorable for DNA preservation over longer periods of time.

Our microbial abundance results showed that storage in warm aerobic conditions greatly altered the composition of the microbial communities since clear environmental clustering of microbial profiles could only be observed using sequence data from to samples stored in controlled conditions. It is possible that such storage conditions also accelerated the decay of ancient wood remains as various microbial taxa involved in the degradation of lignin, cellulose or lignin-derived aromatic compounds could be identified (Taylor 1983; Harwood & Gibson 1988; Song *et al.* 2013; Tsuji *et al.* 2015; Kato *et al.* 2015). Further work is, however, required before the exact impact of storage conditions on DNA preservation levels can be assessed, and biomarkers of molecular DNA degradation based on taxonomic composition of microbiota can be developed.

We provide the first clear molecular evidence for the authenticity of aDNA extracted from wood at the nucleotide level reflected in typical post-mortem damage patterns, small fragment sizes and progressive DNA decay over a period of 8.7 thousand thermal years. Post-mortem cytosine deamination rates within single-stranded overhangs tended to increase with age and were found

saturated from approximately 5 thousand thermal years ago. We found that the DNA fragment size was linearly correlated with thermal age but that other factors can be expected to impact the rate of depurination-driven DNA fragmentation in waterlogged environments (Corinaldesi *et al.* 2008). We uncovered similar decay kinetics for organellar and nuclear DNA which is in agreement with findings made for herbarium specimen (Weiß *et al.* 2016) but contrasts with results on bone material (Schwarz *et al.* 2009; Allentoft *et al.* 2012; Kistler *et al.* 2015, 2017). Consistent with the presence of heterogeneous microenvironmental conditions driving DNA decay as formerly reported for animals (Allentoft *et al.* 2012), we found a lot of variation between samples of similar age.

In 21 oak samples with a chloroplast DNA coverage >5X, we identified ancient chloroplast haplotypes from Neolithic sites in Switzerland (Bieler See, Eschenz Orkopf) and Slovenia (Strojanova voda, Spica), Bronze Age sites in Germany (Unteruhldingen) and France (Erstein), and Medieval sites from northern Germany and northern France (Hamburg, Greifswald, Champeaux). All of these haplotypes matched the most frequent haplotypes present in nearby modern populations. This pattern is compatible with a continuity of the maternally-transmitted lineages within these areas. In the absence of sufficient nuclear DNA data, this pattern is, however, not sufficient to establish continuity and does not allow us to rule out alternative scenarios, such as cross-regional movements within the range of the respective haplotype distributions. Given the limited evolutionary rate of the chloroplast genome, it is highly unlikely that even a single of the 34 nucleotide sites used for defining haplogroup can be affected by a mutational event. Hence, populations that split a few centuries and/or millennia ago can show identical chloroplast haplotypes, thereby limiting our capacity to disentangle local and non-local origins from chloroplast DNA information. Additionally, the geographic and temporal range for which chloroplast DNA data could be collected is admittedly limited, and not sufficient to test whether the genetic structure of modern population was already established during the Early Holocene (Petit *et al.* 2002b). Future large-scale screenings of both nuclear and chloroplast aDNA should aim at charting ancient haplotype distributions through space and time, in order to clarify geographical origin and timing of human-induced translocations (König *et al.* 2002; Lowe *et al.* 2004; Wagner *et al.* 2015a).

Future work should undertake the characterize sufficient amount of nuclear DNA variation before

formal continuity tests such as those developed by Rasmussen and colleagues (Rasmussen *et al.* 2014) can be implemented. For now, we note that pollen, charcoal and/or tree-rings data available in the western Lake Constance area, where two of our study sites are located (Unteruhldingen, 3.7 thousand years, and Eschenz-Orkopf, 5.2 thousand years), suggest that oak populations expanded into *Corylus*-dominated woodland seven to eight thousand years ago (Fig. 6). Early Neolithic forest clearance (cutting, burning) then promoted the expansion of beech and a decrease in the size of the oak population. Future characterization of nuclear data will help determine whether the ancient wood remains collected from Eschenz Orkopf and Unteruhldingen presumably originated from remaining sources of oaks following human-driven coppicing and clearings during the Neolithic and Bronze Age (Fig. 6, (Billamboz 2014; Billamboz & Martinelli 2015)), or by the short-distance movements of acorns from nearby stands.

In conclusion, our study highlights the potential value of waterlogged wood as a source of ancient tree DNA. The methodology described paves the way for large-scale paleogenomic investigations of temperate trees and the genetic consequences of environmental changes during the Holocene. These results open up new possibilities for discovering ancient phylogeographic patterns and micro-evolutionary trajectories in trees, and for improving conservation strategies for cultural heritage items composed of wood.

Brandt for discussions and assistance. Site permissions were obtained for Lucone from the *Ministero dei beni e delle attività culturali e del turismo* (Prot. N 993 Cl. 34.07.19,f.2) and for Viverone from the *Direzione regionale per i beni culturali e paesaggistici del Piemonte* (Prot. 773 cl. 34.16.1919.2).

Author contributions

Conceived and designed the experiments: SW, AK and LO. Performed the experiments: SW and ASO, with input from LO. Analyzed the data: SW and LO. Contributed materials/experimental/analysis tools: SW, FL, MS, TL, EG, EC, IBH, VB, AB, CB, YB, MB, CC, KC, FE, UH, JK, FL, FL, CL, NM, GM, ON, AP, RP, MR, RS, HS, WT, XT, FV, AK and LO. Wrote the paper: SW, CP, AK and LO.

References

Aguilera M, Ferrio Díaz JP, Araus Ortega JL, Tarrús J, Voltas Velasco J (2011) Climate at the onset of western Mediterranean agriculture expansion: Evidence from stable isotopes of sub-fossil oak tree rings in Spain. *Palaeogeography, Palaeoclimatology, Palaeoecology*, **299**, 541–551.

Aitken SN, Yeaman S, Holliday JA, Wang T, Curtis-McLane S (2008) Adaptation, migration or extirpation: climate change outcomes for tree populations. *Evolutionary Applications*, **1**, 95–111.

Allentoft ME, Collins M, Harker D *et al.* (2012) The half-life of DNA in bone: measuring decay kinetics in 158 dated fossils. *Proceedings. Biological sciences / The Royal Society*, **279**, 4724–4733.

Becker B (2006) An 11,000-year German oak and pine dendrochronology for radiocarbon calibration. *Radiocarbon*, **35**, 201–213.

Becker B, Kromer B, Trimborn P (1991) A stable-isotope tree-ring timescale of the Late Glacial/Holocene boundary. *Nature*, **353**, 647.

Billamboz A (2014) Regional patterns of settlement and woodland developments: Dendroarchaeology in the Neolithic pile-dwellings on Lake Constance (Germany). *The Holocene*, **24**, 1–10.

Billamboz A, Martinelli N (2015) Dendrochronology and Bronze Age pile-dwellings on both sides of

the Alps: from chronology to dendrotypoloy highlithing settlement developments and woodland structural changes. In: *The end of the lake-dwellings in the Circum-Alpine region* (ed Menotti F), pp. 68–84. Oxbow books, Oxford and Philadelphia.

Briggs AW, Stenzel U, Johnson PLF *et al.* (2007) Patterns of damage in genomic DNA sequences from a Neandertal. *Proceedings of the National Academy of Sciences of the United States of America*, **104**, 14616–14621.

Büntgen U, Tegel W, Nicolussi K *et al.* (2011) 2500 years of European climate variability and human susceptibility. *Science*, **331**, 578–582.

Cappellini E, Gilbert MTP, Geuna F *et al.* (2010) A multidisciplinary study of archaeological grape seeds. *Naturwissenschaften*, **97**, 205–217.

Cheddadi R, Vendramin GG, Litt T *et al.* (2006) Imprints of glacial refugia in the modern genetic diversity of *Pinus sylvestris*. *Global Ecology and Biogeography,* **15**, 271–282.

Collins MJ, Nielsen–Marsh CM, Hiller J *et al.* (2002) The survival of organic matter in bone: a review. *Archaeometry*, **44**, 383–394.

Corinaldesi C, Beolchini F, Dell'Anno A (2008) Damage and degradation rates of extracellular DNA in marine sediments: implications for the preservation of gene sequences. *Molecular Ecology*, **17**, 3939–3951.

Čufar K, Kromer B, Tolar T, Velušček A (2010) Dating of 4th millennium BC pile-dwellings on Ljubljansko barje, Slovenia. *Journal of Archaeological Science*, **37**, 2031–2039.

Deguilloux MF, Bertel L, Celant A *et al.* (2006) Genetic analysis of archaeological wood remains: first results and prospects. *Journal of Archaeological Science*, **33**, 1216–1227.

Deguilloux M-F, Pemonge M-H, Petit RJ (2002) Novel perspectives in wood certification and forensics: dry wood as a source of DNA. *Proceedings of the Royal Society of London. Series B*, **269**, 1039–1046.

Franks SJ, Weber JJ, Aitken SN (2014) Evolutionary and plastic responses to climate change in terrestrial plant populations. *Evolutionary Applications*, **7**, 123–139.

Frascaria N, Maggia L, Michaud M, Bousquet J (1993) The rbcL gene sequence from chestnut indicates a slow rate of evolution in the Fagaceae. *Genome*, **36**.

Friedrich M, Kromer B, Spurk M, Hofmann J, Felix Kaiser K (1999) Paleo-environment and radiocarbon calibration as derived from Lateglacial/Early Holocene tree-ring chronologies - an intercomparison of *Quercus robur*. *Quaternary International*, **61**, 27.

Friedrich M, Remmele S, Kromer B *et al.* (2004) The 12,460-year Hohenheim oak and pine tree-ring chronology - a unique annual record for radiocarbon calibration and paleoenvironment reconstructions. *Radiocarbon*, **46**, 1111–1122.

Gamba C, Hanghøj K, Gaunitz C *et al.* (2016) Comparing the performance of three ancient DNA extraction methods for high-throughput sequencing. *Molecular Ecology Resources*, **16**, 459–469.

Giguet-Covex C, Pansu J, Arnaud F *et al.* (2014) Long livestock farming history and human landscape shaping revealed by lake sediment DNA. *Nature Communications*, **5**.

Gómez-Zeledón J, Grasse W, Runge F, Land A, Spring O (2017) TaqMan qPCR pushes boundaries for the analysis of millennial wood. *Journal of Archaeological Science*, **79**, 53–61.

Guichoux E, Lagache L, Wagner S, Léger P, Petit RJ (2011) Two highly validated multiplexes (12-plex and 8-plex) for species delimitation and parentage analysis in oaks (*Quercus spp.*). *Molecular Ecology Resources*, **11**, 578–585.

Guichoux E, Petit RJ (2014) Déclaration d'invention (n° DI-RV-13-00566) auprès de l'INPI : Méthode de traçabilité géographique des bois de chêne. *Patent*.

Harwood CS, Gibson J (1988) Anaerobic and aerobic metabolism of diverse aromatic compounds by the photosynthetic bacterium *Rhodopseudomonas palustris*. *Applied and Environmental Microbiology*, **54**, 712–717.

Jónsson H, Ginolhac A, Schubert M, Johnson PLF, Orlando L (2013) mapDamage2.0: fast approximate Bayesian estimates of ancient DNA damage parameters. *Bioinformatics* , **29**, 1682–1684.

Jørgensen T, Haile J, Möller PER *et al.* (2012) A comparative study of ancient sedimentary DNA, pollen and macrofossils from permafrost sediments of northern Siberia reveals long-term vegetational stability. *Molecular Ecology*, **21**, 1989–2003.

Kato S, Chino K, Kamimura N *et al.* (2015) Methanogenic degradation of lignin-derived monoaromatic compounds by microbial enrichments from rice paddy field soil. *Scientific*

Reports, **5**, 14295.

Kistler L, Smith O, Ware R *et al.* (2015) Thermal age, cytosine deamination and the veracity of 8,000 year old wheat DNA from sediments. *bioRxiv*.

Kistler L, Ware R, Smith O, Collins M, Allaby RG (2017) A new model for ancient DNA decay based on paleogenomic meta-analysis. *Nucleic Acids Research*, **45**, 6310–6320.

König AO, Ziegenhagen B, van Dam BC *et al.* (2002) Chloroplast DNA variation of oaks in western Central Europe and genetic consequences of human influences. *Forest Ecology and Management*, **156**, 147–166.

Kremer A, Kleinschmit J, Cottrell J *et al.* (2002) Is there a correlation between chloroplastic and nuclear divergence, or what are the roles of history and selection on genetic diversity in European oaks? *Forest Ecology and Management*, **156**, 75–87.

Lang G (1994) *Quartäre Vegetationsgeschichte Europas: Methoden und Ergebnisse*. Gustav Fischer Verlag, Jena.

Langmead B, Salzberg SL (2012) Fast gapped-read alignment with Bowtie 2. *Nature Methods*, **9**, 357–359.

Lendvay B, Hartmann M, Brodbeck S *et al.* (2017) Improved recovery of ancient DNA from subfossil wood - application to the world's oldest Late Glacial pine forest. *New Phytologist*. doi: 10.1111/nph.14935

Leroy T, Roux C, Villate L *et al.* (2017) Extensive recent secondary contacts between four European white oak species. *New Phytologist*, **214**, 865–878.

Liepelt S, Cheddadi R, de Beaulieu J *et al.* (2009) Postglacial range expansion and its genetic imprints in *Abies alba* (Mill.) - a synthesis from paleobotanic and genetic data. *Review of Palaeobotany and Palynology*, **153**, 139–149.

Liepelt S, Sperisen C, Deguilloux M-F *et al.* (2006) Authenticated DNA from ancient wood remains. *Annals of Botany*, **98**, 1107–1111.

Li H, Handsaker B, Wysoker A *et al.* (2009) The Sequence Alignment/Map format and SAMtools. *Bioinformatics* , **25**, 2078–2079.

Louvel G, Der Sarkissian C, Hanghøj K, Orlando L (2016) metaBIT, an integrative and automated metagenomic pipeline for analysing microbial profiles from high-throughput sequencing shotgun

data. *Molecular Ecology Resources*, **16**, 1415–1427.

Lowe A, Munro R, Samuel S, Cottrell J (2004) The utility and limitations of chloroplast DNA analysis for identifying native British oak stands and for guiding replanting strategy. *Forestry*, **77**, 335–347.

MacDicken K (2015) Special Issue: Changes in Global Forest Resources from 1990 to 2015. *Forest Ecology and Management*, **352**, 1–2.

Magri D (2008) Patterns of post-glacial spread and the extent of glacial refugia of European beech (*Fagus sylvatica*). *Journal of Biogeography*, **35**, 450–463.

Martinelli N (2013) Dendrotypology in Italy: The case studies of the pile-dwelling villages Lucone D (Brescia) and Sabbione (Varese). In: *Dendro: Chronologie, Typologie, Oekologie, Festschrift für André Billamboz zum 65. Geburtstag* (ed Bleicher N), pp. 117–124. Janus Verlag, Freiburg i. Br.

Meyer M, Kircher M (2010) Illumina sequencing library preparation for highly multiplexed target capture and sequencing. *Cold Spring Harbor Protocols*, **2010**, db.prot5448.

Muir G, Fleming CC, Schltterer C (2000) Taxonomy: species status of hybridizing oaks. *Nature*, **405**, 1016.

Nayling N, Manning S, Kromer B *et al.* (2007) Dating the submerged forests: dendrochronology and radiocarbonwiggle-match dating. *CBA Research Reports*, **149**, 90.

Nielsen-Marsh CM, Smith CI, Jans MME *et al.* (2007) Bone diagenesis in the European Holocene II: taphonomic and environmental considerations. *Journal of Archaeological Science*, **34**, 1523–1531.

Orlando L, Gilbert MTP, Willerslev E (2015) Reconstructing ancient genomes and epigenomes. *Nature reviews. Genetics*, **16**, 395–408.

Palla F, Barresi G, Di Carlo E (2014) Identification of bacterial taxa in archaeological waterlogged wood. *Conservation Science in Cultural Heritage*, **14**, 247–254.

Parducci L, Jørgensen T, Tollefsrud MM *et al.* (2012) Glacial Survival of Boreal Trees in Northern Scandinavia. *Science*, **335**, 1083–1086.

Parducci L, Suyama Y, Lascoux M, Bennett D (2005) Ancient DNA from pollen: a genetic record of population history in Scots pine. *Molecular Ecology*, **14**, 2873–2882.

Pedersen NB (2015) Microscopic and spectroscopic characterisation of waterlogged archaeological softwood from anoxic environments. *Thesis.* University of Copenhagen.

Pedersen MW, Ruter A, Schweger C *et al.* (2016) Postglacial viability and colonization in North America's ice-free corridor. *Nature*, **537**, 45–49.

Petit RJ, Csaikl UM, Bordács S *et al.* (2002a) Chloroplast DNA variation in European white oaks: Phylogeography and patterns of diversity based on data from over 2600 populations. *Forest Ecology and Management*, **156**, 5–26.

Petit RJ, Simon B, Sándor B *et al.* (2002b) Identification of refugia and post-glacial colonisation routes of European white oaks based on chloroplast DNA and fossil pollen evidence. *Forest Ecology and Management*, **156**, 49–74.

Pinhasi R, Fernandes D, Sirak K *et al.* (2015) Optimal Ancient DNA Yields from the Inner Ear Part of the Human Petrous Bone. *PloS One*, **10**, e0129102.

Plomion C, Aury J-M, Amselem J *et al.* (2016) Decoding the oak genome: public release of sequence data, assembly, annotation and publication strategies. *Molecular Ecology Resources*, **16**, 254–265.

Plomion C, Leprovost G, Stokes A (2001) Wood formation in trees. *Plant Physiology*, **127**, 1513–1523.

Pollmann B, Jacomet S, Schlumbaum A (2005) Morphological and genetic studies of waterlogged *Prunus* species from the Roman vicus Tasgetium (Eschenz, Switzerland). *Journal of Archaeological Science*, **32**, 1471–1480.

Rasmussen M, Anzick SL, Waters MR *et al.* (2014) The genome of a Late Pleistocene human from a Clovis burial site in western Montana. *Nature*, **506**, 225–229.

Schlumbaum A, van Glabeke S, Roldan-Ruiz I (2012) Towards the onset of fruit tree growing north of the Alps: ancient DNA from waterlogged apple (*Malus sp.*) seed fragments. *Annals of Anatomy*, **194**, 157–162.

Schmid S, Genevest R, Gobet E *et al.* (2017) HyRAD-X, a versatile method combining exome capture and RAD sequencing to extract genomic information from ancient DNA. *Methods in Ecology and Evolution*.

Schubert M, Ermini L, Sarkissian CD *et al.* (2014) Characterization of ancient and modern genomes by SNP detection and phylogenomic and metagenomic analysis using PALEOMIX. *Nature Protocols*, **9**, 1056–1082.

Schubert M, Ginolhac A, Lindgreen S *et al.* (2012) Improving ancient DNA read mapping against modern reference genomes. *BMC Genomics*, **13**, 178.

Schwarz C, Debruyne R, Kuch M *et al.* (2009) New insights from old bones: DNA preservation and degradation in permafrost preserved mammoth remains. *Nucleic Acids Research*, **37**, 3215–3229.

Schweingruber FH (1990) *Microscopic Wood Anatomy*. Kommissionsverlag Züricher AG.

Segata N, Izard J, Waldron L *et al.* (2011) Metagenomic biomarker discovery and explanation. *Genome Biology*, **12**, R60.

Segata N, Waldron L, Ballarini A *et al.* (2012) Metagenomic microbial community profiling using unique clade-specific marker genes. *Nature Methods*, **9**, 811–814.

Smith CI, Chamberlain AT, Riley MS, Stringer C, Collins MJ (2003) The thermal history of human fossils and the likelihood of successful DNA amplification. *Journal of Human Evolution*, **45**, 203–217.

Smith O, Momber G, Bates R *et al.* (2015) Sedimentary DNA from a submerged site reveals wheat in the British Isles 8000 years ago. *Science*, **347**, 998–1001.

Song N, Cai H-Y, Yan Z-S, Jiang H-L (2013) Cellulose degradation by one mesophilic strain *Caulobacter sp*. FMC1 under both aerobic and anaerobic conditions. *Bioresource Technology*, **131**, 281–287.

Speirs AK, Mc Connachie G, Lowe AJ (2009) Chloroplast DNA from 16th century waterlogged oak in a marine environment: initial steps in sourcing the Mary Rose timbers. *Terra Australis*, **30**.

Tani N, Tsumura Y, Sato H (2003) Nuclear gene sequences and DNA variation of *Cryptomeria japonica* samples from the postglacial period. *Molecular Ecology*, **12**, 859–868.

Taylor BF (1983) Other Methoxy-Aromatic Compounds by Pseudomonas sp. Strain PN-1. *Applied and Environmental Microbiology*, **46**, 1286–1292.

Tegel W, Elburg R, Hakelberg D, Stäuble H, Büntgen U (2012) Early Neolithic water wells reveal the world's oldest wood architecture. *PloS One*, **7**, e51374.

Tollefsrud MM, Kissling R, Gugerli F *et al.* (2008) Genetic consequences of glacial survival and

    postglacial colonization in Norway spruce: combined analysis of mitochondrial DNA and fossil

    pollen. *Molecular Ecology*, **17**, 4119–4135.

Truong DT, Franzosa EA, Tickle TL *et al.* (2015) MetaPhlAn2 for enhanced metagenomic taxonomic

    profiling. *Nature Methods*, **12**, 902–903.

Tsuji Y, Vanholme R, Tobimatsu Y *et al.* (2015) Introduction of chemically labile substructures into

    Arabidopsis lignin through the use of LigD, the Cα-dehydrogenase from *Sphingobium sp*. strain

    SYK-6. *Plant Biotechnology Journal*, **13**, 821–832.

Wagner S, Liepelt S, Gerber S, Petit RJ (2015a) Within-range translocations and their consequences

    in European larch. *PloS One*, **10**, e0127516.

Wagner S, Litt T, Sánchez-Goñi M-F, Petit RJ (2015b) History of *Larix decidua* Mill. (European

    larch) since 130 ka. *Quaternary Science Reviews*, **124**, 224–247.

Wales N, Andersen K, Cappellini E, Ávila-Arcos MC, Gilbert MTP (2014) Optimization of DNA

    Recovery and Amplification from Non-Carbonized Archaeobotanical Remains. *PloS One*, **9**,

    e86827.

Wales N, Ramos Madrigal J, Cappellini E *et al.* (2016) The limits and potential of paleogenomic

    techniques for reconstructing grapevine domestication. *Journal of Archaeological Science*, **72**,

    57–70.

Wales N, Romero-Navarro JA, Cappellini E, Gilbert MTP (2012) Choosing the best plant for the job:

    a cost-effective assay to prescreen ancient plant remains destined for shotgun sequencing. *PloS

    One*, **7**, e45644.

Weiß CL, Dannemann M, Prüfer K, Burbano HA (2015) Contesting the presence of wheat in the

    British Isles 8,000 years ago by assessing ancient DNA authenticity from low-coverage data.

    eLife, **4**.

Weiß CL, Schuenemann VJ, Devos J *et al.* (2016) Temporal patterns of damage and decay kinetics of

    DNA retrieved from plant herbarium specimens. *Open Science*, **3**, 160239.

Willerslev E, Davison J, Moora M *et al.* (2014) Fifty thousand years of Arctic vegetation and

    megafaunal diet. *Nature*, **506**, 47–51.

Data Accessibility

All the sequencing data are available for download from the European Nucleotide Archive under accession number PRJEB21188.

Supplementary Material

Supplementary Figures
"**SI_AncientOak.docx**"
Fig. S1 | Observed chloroplast DNA heterozygosities.
Fig. S2 | Fragment lengths distribution across all samples.
Fig. S3 | Heatmap of microbe species found across all samples.
Fig. S4 | Heatmap of microbe families in samples with highest endogenous DNA content.
Fig. S5 | Principal Coordinate Analysis charts including all samples.
Fig. S6 | Eigenvalues of PCoA for 48 samples stored in controlled conditions.
Fig. S7 | LDA scores obtained for the four main clusters at the genus and species level.
Fig. S8 | DNA degradation patterns.
Fig. S9 | DNA damage plots for nuclear sequences of sample #524 from the Bouldnor Cliff.
Fig. S10 | DNA damage plots for chloroplast sequences of sample #524 from the Bouldnor Cliff.
Fig. S11 | DNA damage plots for nuclear sequences of sample #524 from the Bouldnor Cliff.
Fig. S12 | DNA damage plots for chloroplast sequences of sample #524 from the Bouldnor Cliff.
Fig. S13 | DNA damage plots for nuclear sequences of sample #524 from the Bouldnor Cliff.
Fig. S14 | Comparison of endogenous DNA content of ancient sapwood and heartwood.

Supplementary Text
Text S 1 BouldnorCliffDiscussion (docx)

Supplementary Tables
Table S 1 | Geographic data and ages (xlsx)
Table S 2 | PCR results (xlsx)
Table S 3 | Modern haplotypes (xlsx)
Table S 4 | Endogenous DNA content (xlsx)
Table S 5 | Shannon Indexes (xlsx)
Table S 6 | BouldnorCliff (xlsx)

Table 1 | Summary of ancient wood samples analyzed in this study (ka = kilo-annus). See Supplementary Table 1 for geographical coordinates, dating, storage history and thermal age calculations.

Site	Age [ka]	Thermal Age [ka@10°C]	Collection Year	Taphonomical context	Type of wood	Samples
Amélie	4.5	7.9	2014*	Marine intertidal silts, foreshore	Piles exposed to tides	4
Bouldnor Cliff	8.0	7.0	2015*	Marine submerged peat	Logs, submerged forest	4
Champeaux	1.4	2.3	2015*	Marine intertidal silts, foreshore	Buried piles, fish weir	8
Conjux	2.8	5.2	2014*	Limy lake sediments	Piles, dwellings	5
Droßdorf	7.1	7.8	2014	Terrestrial glacio-fluvial sands	Planks, water well	12
Erstein 204	3.0	4.0	2014	Terrestrial sands and loess on limy bedrock	Planks, water well	5
Erstein 218	3.7	5.0	2014*	Terrestrial sands and loess on limy bedrock	Planks, water well	5
Eschenz Orkopf	5.2	5.4	2015*	Limy lake sediments	Piles, dwellings	9
Etang de Thau	2.8	6.3	2015*	Marine lagoonal sands	Piles	4
Greifswald	0.7	0.5	2014*	Organic wetland sediment	Planks	4
Hamburg	0.5	0.4	2015*	Organic wetland sediment	Planks	8
La Draga	7.1	10.0	2014	Peat and limy lake sediments	Piles, dwellings	9
Le Gurp	9.8	14.0	2014*	Coastal peat and sands	Logs, buried forest	4
Lillemer	5.8	13.8	2015*	Black peat	Logs, buried forest	4
Lucone	4.0	7.0	2014	Peat (gyttja)	Piles, dwellings	9
Ludwigshafen Holzplatz	5.2	5.4	2009-2014	Limy lake sediments	Piles, dwellings	12
Reims	1.7	1.5	2008	Clay	Piles	3
Rødby	6.9	5.9	2015*	Peat (gyttja)	Logs, buried forest	4
Saint Loup de Varennes	1.9	2.5	2014	Clay	Planks	3
Spica	4.5	7.8	2010	Marsh and limy lake sediments	Piles, dwellings	7
Strojanove vode	5.6	8.7	2012	Marsh and limy lake sediments	Piles, dwellings	9

Sutz Lattringen Ruette	4.7	5.6	2014	Limy lake sediments	Piles, dwellings	14
Unteruhldingen site 1	3.7	4.8	2016*	Limy lake sediments	Piles, dwellings	3
Unteruhldingen site 2	2.9	3.8	2016*	Limy lake sediments	Piles, dwellings	4
Viverone	3.4	6.9	2011	Lacustrine sands	Piles, dwellings	10
Vicus Tasgetium	2.0	3.4	2012	Clay	Planks	4

* controlled storage: vacuum-packed and at 4°C.

Table 2 Samples with highest final coverages achieved in this study. U: USER treated libraries.

Sample ID	Site	Retained sequences	Chloroplast coverage	Nuclear coverage [%]
546	Unteruhldingen site 1	1.35E+07	47.98	14.34
382 U	Hamburg	1.36E+07	36.45	10.32
384 U	Hamburg	3.23E+07	18.64	10.13
049	Erstein 218	1.09E+07	17.03	1.47
423 U	Greifswald	1.53E+07	16.41	8.89
442 U	Eschenz Orkopf	4.71E+08	16.22	1.41
044 U	Erstein 218	2.57E+07	15.98	1.55
235 U	Sutz Lattrigen Ruette	9.56E+07	15.47	6.05
045	Erstein 218	4.63E+07	15.17	2.85
233 U	Sutz Lattrigen Ruette	7.16E+07	14.99	1.08
447 U	Eschenz Orkopf	2.10E+08	14.92	4.31
046 U	Erstein 218	2.34E+07	14.76	3.52
379	Hamburg	7.35E+06	12.79	5.74
321 U	Spica	2.31E+08	12.12	1.06
354 U	Strojanove vode	6.07E+07	12.01	1.14
548	Unteruhldingen site 1	1.01E+07	10.41	13.53
466 U	Champeaux	4.37E+07	10.34	2.64
469	Champeaux	1.85E+07	9.47	0.46
542	Erstein 204	2.55E+07	8.57	1.05
016	Eschenz Orkopf	5.48E+07	6.72	3.17
435	Hamburg	7.59E+06	5.86	2.72
523 U	Bouldner Cliff 2	3.08E+08	3.36	**0.03**
438	Hamburg	6.30E+06	2.37	2.41

048	Erstein 218	1.27E+07	2.34	0.34
543	Erstein 204	2.17E+07	2.28	0.97
552	Unteruhldingen site 2	9.15E+06	1.76	0.26
462	Champeaux	6.22E+06	1.53	0.09
381	Hamburg	6.68E+06	1.52	0.59
401	Ludwigshafen Holzplatz	1.48E+07	1.11	0.13
496	Etang de Thau	1.32E+07	1.09	0.08

a

Microbe Abundances

10^{-2} 10^{-2} 10^{-0} 10^{1}

Endogenous oak
Taphonomical context
Site

Methanobacterium sp SWAN1
Methanobacterium spec.
Methanocella spec.
Methanomassiliicoccus luminyen
Methanosaeta concilii
Methanosaeta spec.
Methanosarcina spec.
Deinococcus spec.
Oenococcus oeni
Zymophilus raffinosivorans
Asticcacaulis spec.
Brevundimonas spec.
Caulobacter spec.
Caulobacter vibroides
Rhodopseudomonas palustris
Rhodopseudomonas spec.
Celeribacter baekdonensis
Azospirillum spec.
Rhodosprillum spec.
Sphingobium spec.
Sphingobium xenophagum
Burkholderia spec.
Thiomonas spec.
Limnohabitans spec.
Polaromonas spec.
Variovorax spec.
Janthinobacterium spec.
Massilia spec.
Sulfuricella denitrificans
Thiobacillus thioparus
Methylotenera mobilis
Methylotenera spec.
Desulfomonile tiedjei
Arcobacter spec.
Sulfurimonas spec.
Marinobacter spec.
Shewanella frigidimarina
Shewanella spec.
Rheinheimera spec.
Methylocater tundripaludum
Methylocater spec.
Marinomonas spec.
Thalassolituus oleivorans
Pseudomonas sp GM24
Pseudomonas stutzeri
Pseudomonas spec.
Methylophaga spec.
Rhodobacter spec.
Vicia cryptic virus
Dasheen mosaic virus

Samples

Endogenous oak [%]
- >10
- 1-5
- 5-10
- <1

Taphonomical context
- Organic wetland sediment
- Limy lake sediments
- Sand and loess on limy bedrock
- Coastal peat and sands
- Marine submerged peat
- Marine lagoonal sands
- Marine intertidal silts

Localities
- Bouldnor Cliff 2
- Bouldnor Cliff 5
- Champeaux
- Conjux
- Erstein 208
- Eschenz Orkopf
- Etang de Thau
- Greifswald
- Hamburg
- Le Gurp
- Unteruhldingen 1
- Unteruhldingen 2

b

- Organic wetland sediments
- Limy lake sediments
- Sand and loess on limy bedrock
- Coastal peat and sands
- Marine submerged peat
- Marine lagoonal sands
- Marine intertidal silts

Dimension 3 (9.01%)
Dimension 2 (11.68%)
Dimension 1 (14.05%)

c

- Organic wetland sediments
- Marine sediments
- Loess and sands on limy bedrock
- Limy lake sediments

phyla
classes
orders
families

Bacteroidetes   Actinobacteria
Euryarchaeota
Proteobacteria

h: Methanomicrobia
g: Methanosarcinales
e: Methanosaetaceae
x: Sphingomonadaceae
y: Sphingomonadales
c2: Xanthomonadales
c1: Xanthomonadaceae
l: Actinobacteria
t: Rhodobiaceae
b4: Halomonadaceae
i: Actinomycetales
j: Solirubrobacteriales spec.
k: Solirubrobacteriales
m: Sphingobacteriaceae
o: Sphingobacteria
n: Sphingobacteriales
s: Phyllobacteriaceae
c3: Gammaproteobacteria
b1: Alteromonadales
b0: Shewanellaceae
a8: Campylobacterales
a9: Epsilonproteobacteria
a7: Campylobacteraceae
b5: Oceanospirillaceae
w: Rhodobacterales
v: Rhodobacteraceae
b9: Thiotrichales
b8: Piscirickettsiaceae
a6: Betaproteobacteria
a3: Burkholderiales
b7: Pseudomonadales
b6: Pseudomonadaceae
a4: Methylophilaceae
a5: Methylophilales
a2: Oxalobacteraceae
c0: Sinobacteriaceae
z: Alphaproteobacteria
a1: Comamodaceae
b: Methanocellales
a: Methanocellaceae
q: Caulobacterales
p: Caulobacteraceae
d: Methanomicrobiales
c: Methanoregulaceae
u: Rhizobiales
a0: Burkholderiales
b2: Methylococcaceae
r: Bradyrhizobiaceae
b3: Methylococcales
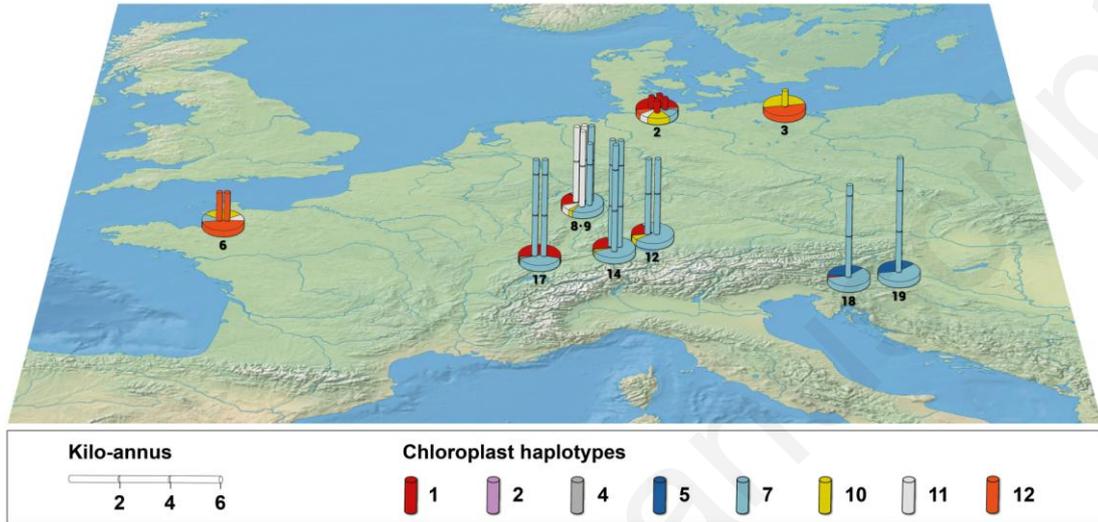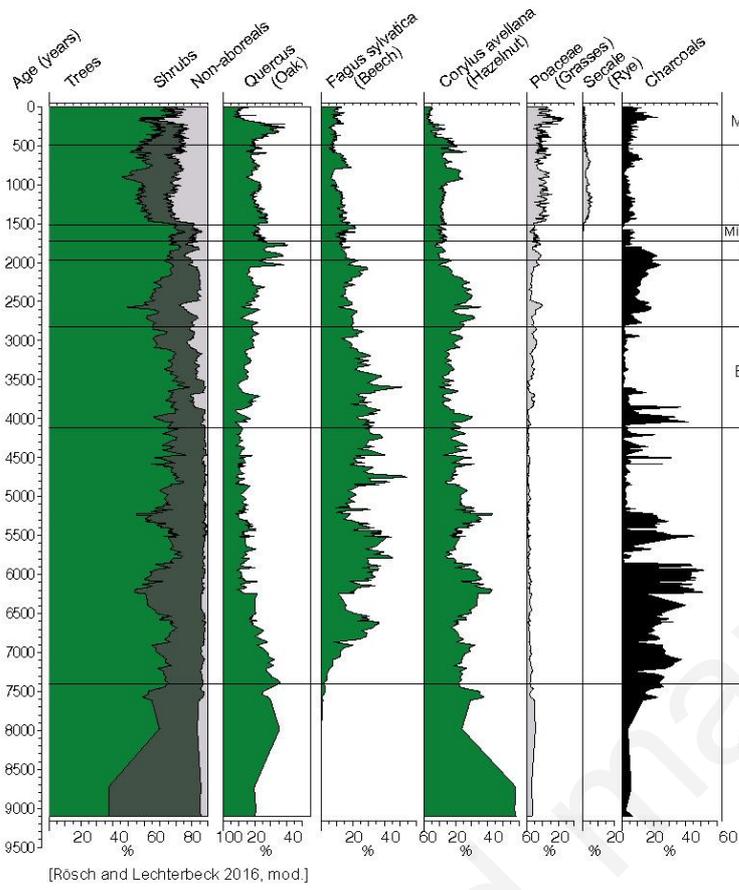f: Methanosarcinaceae

LDA SCORE (log 10)
0   1   2   3   4   5   6

a

Pollen and Charcoals
Litzelsee

b

Chloroplast   Dendrotypology
haplotypes   Western Lake Constance

Age (years)
Trees
Shrubs
Non-aboreals
Quercus (Oak)
Fagus sylvatica (Beech)
Corylus avellana (Hazelnut)
Poaceae (Grasses)
Secale (Rye)
Charcoals

Ha07
Ha01
Ha10
Others

Dendo-groups Upper Lake
Dendo-groups Lower Lake
Age (years)

Modern Age
Medieval
Migration Period
Roman Age
Iron Age
Bronze Age
Neolithic
Mesolithic

0
500
1000
1500
2000
2500
3000
3500
4000
4500
5000
5500
6000
6500
7000
7500
8000
8500
9000
9500

20 40 60 80
%
100 20 40
%
20 40
%
60 20 40
%
60 20
%
20 40
%
20 40 60
%

-3000
-3500
-4000
-4500
-5000
-5500
-6000

Stand thinning
Coppice
Clearings in dense stands

[Rösch and Lechterbeck 2016, mod.]

[Billamboz and Martinelli 2015, mod.
Billamboz 2014, mod.]